Mechanical Engineering Advances 2024, 2(2), 1470.
https://doi.org/10.59400/mea.v2i2.1470

Article

Hydrogel 3D printing with direct and indirect extruder

Thanh Tan Nguyen[1], Ngoc Hieu Pham[1], Hoang Son Tran[1], Le Nguyen Cao[1], Thi Hong Nga Pham[1], Quoc Bao Phan[2], Van Tron Tran[1,*]

[1] Faculty of Mechanical Engineering, Ho Chi Minh City University of Technology and Education, Ho Chi Minh City 71307, Vietnam
[2] Advanced Manufacturing Center, Binh Duong University, Binh Duong province 75000, Vietnam
*** Corresponding author:** Van Tron Tran, trontv@hcmute.edu.vn

CITATION

Nguyen TT, Pham NH, Tran HS, et al. Hydrogel 3D printing with direct and indirect extruder. Mechanical Engineering Advances. 2024; 2(2): 1470.
https://doi.org/10.59400/mea.v2i2.1470

ARTICLE INFO

Received: 24 June 2024
Accepted: 6 September 2024
Available online: 29 October 2024

Abstract: The advancement of additive manufacturing technology or 3-Dimesion printing (3D printing) allows for the creation of parts with intricate designs, resulting in less material waste compared to conventional manufacturing methods. Although current 3D printers primarily use plastic or metal materials, there is a growing interest in using biomaterials for 3D printing. To facilitate this trend, developing and designing 3D printers capable of using hydrogel materials is crucial. In this research, the 3D printer with direct and indirect extruders for hydrogel material is designed, calculated, and manufactured. Then, the 3D printer is tested with conductive sodium alginate 5% + 5% activated carbon by weight. In addition, the electrical conductivity of the material is measured. Through meticulous research and development, a 3D printer capable of printing hydrogel materials has been successfully manufactured, setting the stage for further exploration and the creation of environmentally friendly 3D biomedical printing materials.

Keywords: hydrogel; additive manufacturing; biomaterial; design; manufacture; direct and indirect extruder

1. Introduction

Hydrogels are three-dimensional networks of hydrophilic polymers that can rapidly absorb and retain substantial amounts of water or other liquids [1,2]. These versatile materials are highly flexible and responsive to their environment, making them valuable across various biomedical industries including drug delivery, wound healing, valve and tissue engineering, and sensor applications Hydrogels have gained popularity due to their unique properties, such as high-water retention, softness, flexibility, biocompatibility, responsiveness to temperature, and cost-effectiveness [3,4].

Hydrogel material plays a crucial role in tissue engineering, and the development of hybrid hydrogels using different polymers is a research focus [4]. Their applications range from regenerative medicine to tissue engineering, including bone regeneration, cartilage and vascular tissue engineering, heart-related applications, wound healing, and artificial cornea development. Their biocompatibility, adjustable viscosity, physical and mechanical properties, ability to provide a framework for various tissues, high water content, and oxygen permeability make them highly suitable for these applications [5–7]. There are many ways to synthesize hydrogels such as shear forces, magnetic and electric fields, compression and stretching forces, directional crystallization, ion diffusion, photolithography, and 3D printing [8].

Furthermore, additive manufacturing is an innovative manufacturing technique that creates three-dimensional objects by adding successive layers of material based

on a digital blueprint. Using 3D printing technology with hydrogel materials presents an opportunity to manufacture flexible designs and other complex structures. This advancement may introduce a shift from traditional plastic materials in 3D printing and pave the way for flexible materials to replace plastics, representing a significant breakthrough in 3D printing technology (**Figure 1**).

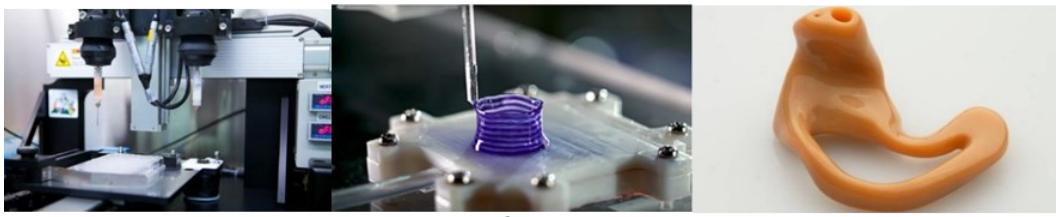

a b c

Figure 1. (a) 3D printing technology using hydrogel materials; **(b)** 3D printing hydrogel to create human body tissues; **(c)** 3D printed artificial ears using flexible materials.

The growth of the additive manufacturing industry is attributed to the opportunities it presents in producing supportive medical items such as artificial organs, implants, surgical guides, and assistive devices. Hydrogel materials, particularly in the production of coronary stents, are widely used in the medical field. Looking ahead, the research and development of 3D printers for hydrogel materials are expected to be a strategic focus. As the manufacturing industry continues to seek innovative and creative directions, 3D printing technology is seen as a transformative tool in the era of Industry 4.0. Exploring various 3D printing technologies and materials, hydrogel biomaterials show promise for producing flexible components. Hence, the development of a liquid material 3D printer and the preparation of hydrogel materials for liquid 3D printing are crucial. Experimental manufacturing and thorough evaluation of printed products will be essential for future research. In this research, the design and manufacture of the 3D printer with direct and indirect extruders was implemented. In addition, conductive sodium alginate 5% + 5% activated carbon by weight material was evaluated in this 3D printer.

2. Material and methods

2.1. Material

Hydrogel: conductive sodium alginate 5% by weight + 5% activated carbon by weight.

Sodium alginate (Na-alginate, viscosity 80–120 cP) was purchased from FUJIFILM Wako Pure Chemical Corporation, Japan. Charcoal (Steam-activated) was purchased from Duchefa Biochemie (Netherlands). Food coloring was bought from KUPKACE SHOP Ltd., Vietnam. All chemicals were used as received without further purification. Distilled water was used for gel preparation

2.2. Sample preparation procedure

Prepare sodium alginate solution using sodium alginate, distilled water, activated carbon and food coloring (**Figure 2**).

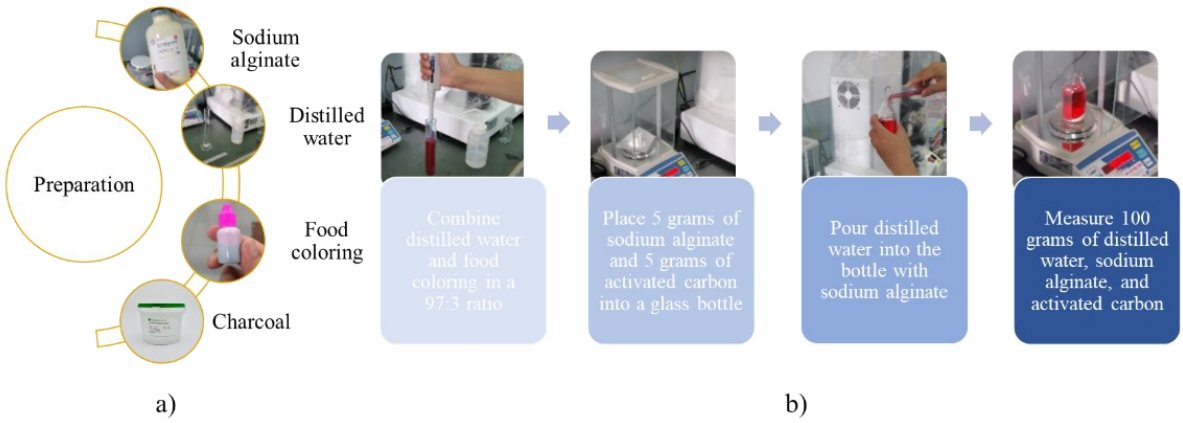

Figure 2. Preparation of materials for making hydrogel.

First, combine distilled water and food coloring in a 97:3 ratio. Second, place 5 grams of sodium alginate and 5 grams of activated carbon into a glass bottle. Next, pour distilled water into the bottle with sodium alginate. Then, measure 100 grams of distilled water, sodium alginate, and activated carbon. Subsequently, stir the solution containing water, charcoal, and alginate twice a day for 3–4 days.

3. Design and calculation

3D printers are often built with 3-axis Cartesian *X*, *Y*, *Z*, Delta, and Polar coordinates. Cartesian structures have the primary benefit of being less expensive than other structure types that have comparable accuracy and repeatability in additive manufacturing [9]. For this project, the Cartesian structure is chosen and managed by the Arduino Mega 2560 circuit, which controls the stepper motor driver of the extruder and the three axes *X*, *Y*, and *Z*. The driver regulates the stepper motor of each axis using lead screw transmission mechanisms-nuts, guide belts, and slide rails to facilitate the movement of the three axes to the desired positions. The machine's hardware is composed of *X*, *Y*, and *Z* axes and dual print heads actuated by stepper motors. Individual axis movements are controlled by drivers, with overall operation managed by an Arduino Mega 2560. Printer settings are displayed on a 2004 LCD panel. The printer communicates with a computer via a USB interface (see **Figure 3**) [10–14].

The process of extrusion in 3D printing technology is facilitated by two primary components: the printer, which regulates the position of the print head, and the extruder, which controls the flow of material. The extrusion system encompasses three main types: a drive screw motor that propels the piston, compressed air that propels the piston, and a drive-through screw that extracts material from an external source. In the drive screw motor system, where the piston is propelled, direct contact is established between the material and the piston. This mechanism effectively governs the extrusion speed due to consistent volume displacement. However, one drawback of this approach is the requisite time to compensate for material loss in the needle tip, potentially leading to imprecise printing.

Alternatively, the pneumatic extrusion system harnesses compressed air as the driving force for extrusion. While compressed air is the more commonly employed medium, nitrogen may be utilized when sterility is necessary, particularly in bio-ink printing applications. Pneumatic extrusion demonstrates proficiency in extruding a

diverse array of viscoelastic objects while boasting rapid response times facilitated by the swift pressurization and depressurization of the tank. Notwithstanding its efficacious performance, this system is comparatively intricate to construct and operate relative to motor control-based systems due to its reliance on compressed air.

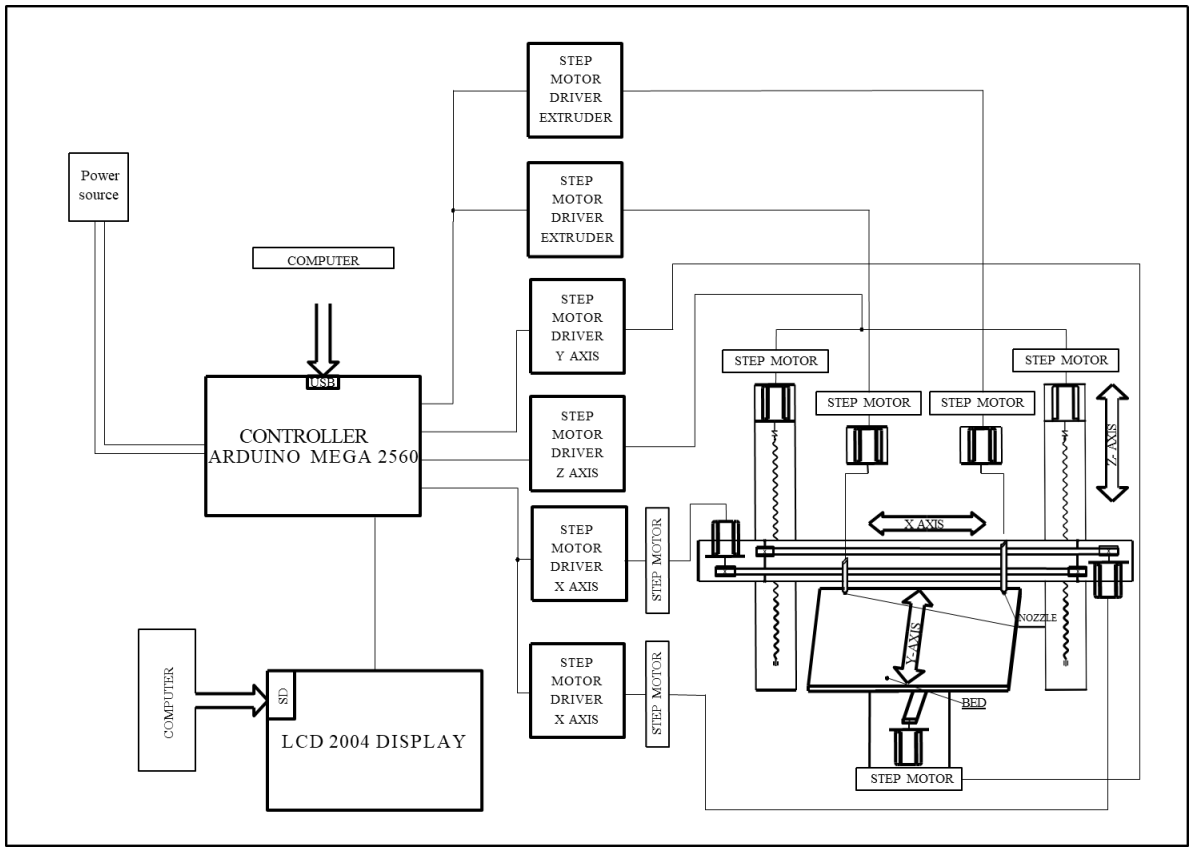

Figure 3. Diagram illustrating the operating principle of a 3D printer.

Lastly, the screw extrusion system engages a singular screw extruder to convey material from the hopper to the nozzle. A notable advantage of this design is its ability to facilitate continuous printing, as material can be loaded on demand. Furthermore, the rotating screw aids in homogenizing the material during the printing process, promoting uniformity and mitigating phase separation. Nevertheless, this design presents potential challenges, such as the risk of cross-contamination, as materials necessitate separate storage containers. Furthermore, delicate materials, such as cells, are unsuitable for screw extrusion transport, as the shear force incurred may compromise the integrity of the cell membrane. Moreover, the extruder design provides two options: direct and indirect extrusion, each accompanied by distinct advantages and disadvantages, as depicted in **Figure 4** and **Table 1**, respectively.

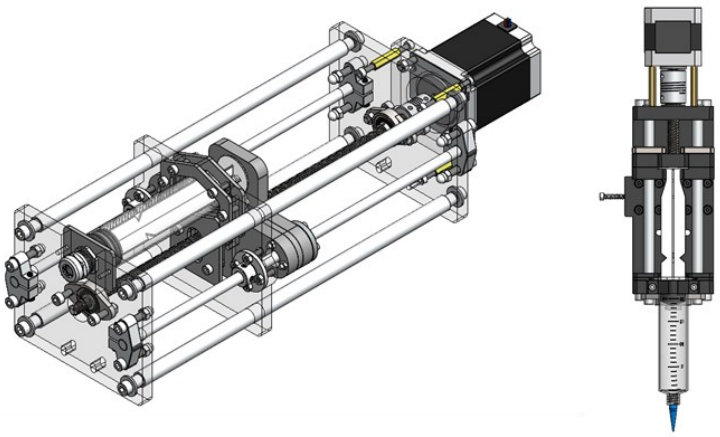

a) b)

Figure 4. Design option. **(a)** Indirect extruder; **(b)** direct extruder.

Table 1. Advantages and disadvantages of Direct and indirect extruders [15–19].

Design method	Advantages	Disadvantages
Indirect extruder	• Large capacity • Does not limit the operating space of the machine • Movement is smoother because the *X*-axis does not have an extruder attached, and only the extruder head is attached.	• Need a motor with high torque. • Slow response time due to friction of the material in the tube. • Extrusion is unstable due to the impact of a large shear force.
Direct extruder	• Stable extrusion • Better material withdrawal • The engine has less power • Less affected by shear stress	• Increasing the *X*-axis mass leads to a limitation in printing speed. • Small storage capacity. • Limit the machine's working space.

This study designed and calculated a combination of direct and indirect extrusion as follows:

Calculate the *X*-axis:

X-axis parameters:

+ Load mass mounted on the *Y* axis: $m_1 = 1.5(\text{kg})$

+ Working length: L=100 (mm)

+ Maximum speed: $v_{max} = 120\ \text{mm/s}$

+ Printing speed: $v_{in} = 60\ \text{mm/s}$

+ Working time: $t = 2$ h

Calculate and select the stepper motor:

Pulley attached to the engine with parameters:

+ Number of teeth: $z = 20$

+ Pitch: $p = 2(\text{mm})$

The achievable maximum speed: v_{max}

→ Pulley's angular speed:

$$\omega_{in} = \frac{v_{in}}{d/2} = \frac{120}{4.75} \approx 25(\text{r/s}) \quad (1)$$

→ Time to rotates 1 round: $t = \frac{1}{25}(\text{s})$.

Distance traveled by the belt when Pulley rotates 1 round:

$$s = z \times p = 20 \times 2 = 40(\text{mm}) \tag{2}$$

Maximum speed of stepper motor:

$$V = \frac{s}{t} = \frac{40(\text{mm})}{\frac{1}{25}(\text{s})} = \frac{40(\text{mm})}{\frac{1}{25} \times \frac{1}{60}(\text{min}())(mm/\text{min}())} \tag{3}$$

$$V = \frac{60000}{40}\left(\text{r/min}()(\text{r/min}())\right) \tag{4}$$

The selected stepper motor is Nema 17 (model KH4238–B90201) with a rated current of 1.2A and voltage of 24V. Maximum rotation speed of the engine is $V = 1500(\text{r/min}())$. The torque of the stepper motor is $M = 125(\text{mN. m})$.

The motor power:

$$P = V.M = 125 \times 10^{-3}.\frac{1500}{60} = 3.125(\text{W}) \tag{5}$$

with: V–motor rotation speed (r/s); M–torque (N. m).

The overall performance of the drive system: $\eta = 0.95$.

Motor working capacity:

$$P_{lv} = \frac{P}{\eta} = \frac{3.125}{0.95} = 3.29(\text{W}) \tag{6}$$

Using the same calculation method, the calculation parameters for the Y and Z axes are respectively $P_{lv} = 3.28(\text{W})$, $P_{lv} = 1.89(\text{W})$, extruder motor is $P_{lv} = 3.15(\text{W})$.

Figure 3 illustrates the printer's operating principle in detail. **Figure 5** presents a detailed block diagram of the hardware components. The mechanical design for the indirect and direct extruder options is shown in **Figure 6**.

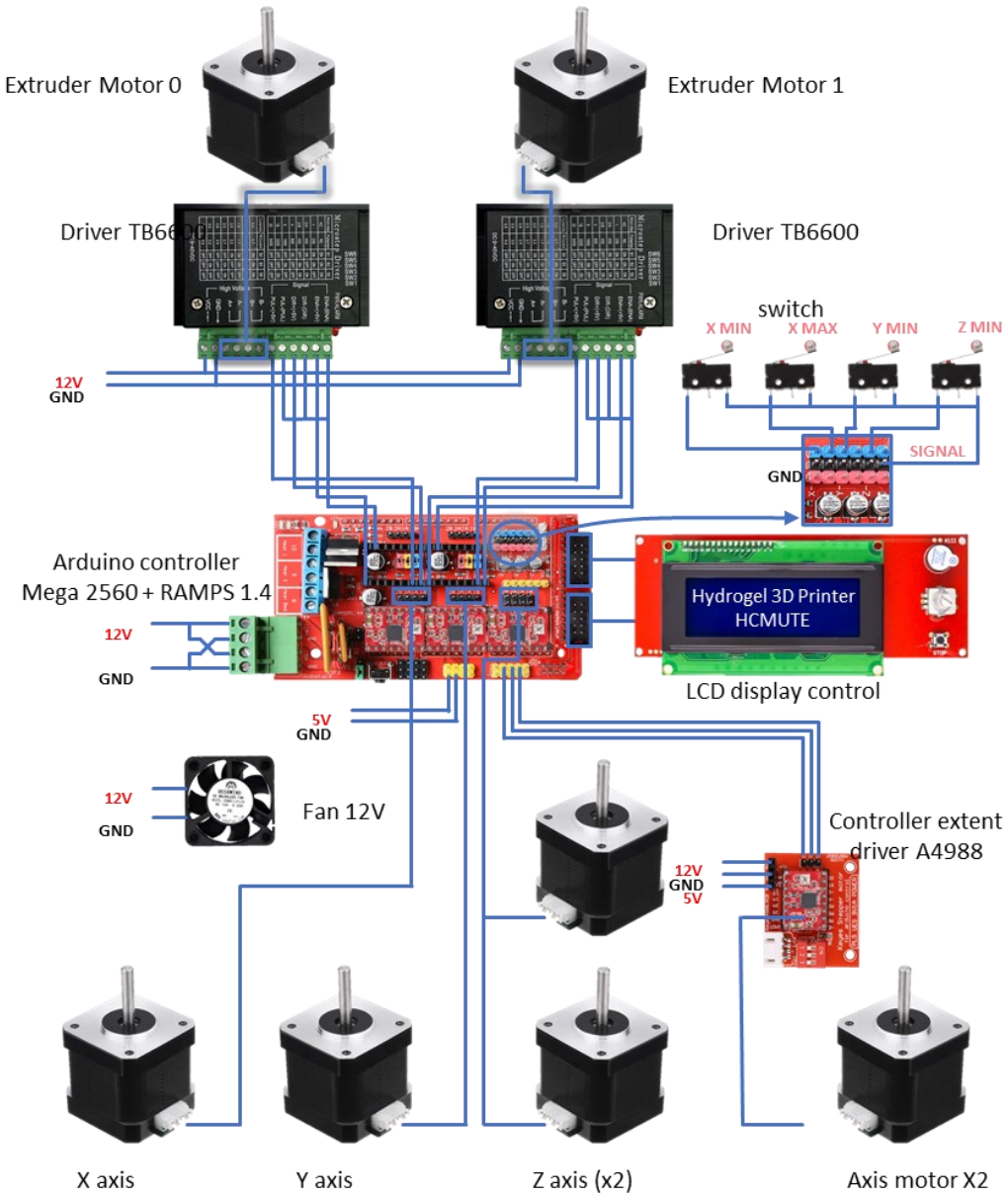

Figure 5. Control block wiring diagram.

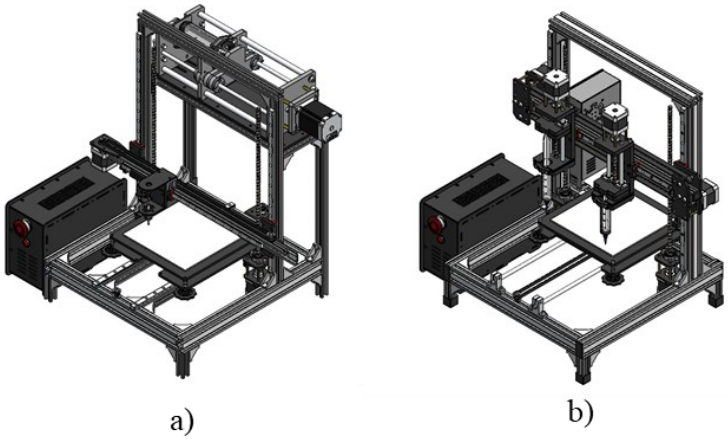

Figure 6. Designed of the 3D printer with. **(a)** Indirect extrusion; **(b)** direct extrusion.

Calculate the hydrogel extruder

Calculate and select screws and nuts:

Input parameters:

+ Volume of cylinder: $V = 20(ml) = 0.02(dm^3)$

+ Specific gravity of gel: $d = 625000(N/m^3)$

+ Average axial force:

$$F_a = Vd = 0.02 \times 10^{-3} \times 625000 = 12.5(N) \quad (7)$$

+ Travel route: L = 150 (mm)

Calculate the average diameter according to the formula:

$$d_2 \geq \sqrt{\frac{F_a}{\pi \psi_H \psi_h [q]}} \quad (8)$$

With $\psi_H = 2.0$ (raw nut); square thread height coefficient $\psi_h = 0.5$; The allowable pressure depends on the material of the screw and nut, we have the material of the screw - nut being steel - brass, choose $[q] = 10(\text{MPa})$.

$$d_2 \geq \sqrt{\frac{12.5}{3.14 \times 2 \times 0.5 \times 10}} \rightarrow d_2 \geq 0.63(\text{mm}) \quad (9)$$

Select $d_2 \approx 7(\text{mm})$, screw pitch $p = 2(\text{mm})$

Select thread parameters:

Thread profile height:$h = 0.1.\, d_2 = 0.1 \times 7 = 0.7(\text{mm})$

Outer diameter: $d = d_2 + h = 7 + 0.7 = 7.7(\text{mm})$

Inner diameter: $d_1 = d_2 - h = 7 - 0.7 = 6.3(\text{mm})$

Thread step: $p = 2h = 2 \times 0.7 = 1.4(\text{mm})$

Screw step: $p_h = Z_h p = 4 \times 1.4 = 5.6(\text{mm})$

Screw angle: $\gamma = arctg[p_h/(\pi d_2)] = arctg\left[\frac{5.6}{\pi \times 7}\right] = 0.25°$

The friction coefficient of the poorly lubricated steel-brass material pair is $f = 0.1$, so $\varphi = \text{arctg}(0{,}1) = 3.64°$.

Through the calculated parameters of the thread, we choose the T8 lead screw with the following parameters:

+ Outside diameter: $d = 8(\text{mm})$

+ Thread profile height: $h = 1(\text{mm})$

+ Average diameter: $d_2 = d - h = 8 - 1 = 7(\text{mm})$

+ Inner diameter: $d_1 = d_2 - h = 7 - 1 = 6(\text{mm})$

+ Thread step: $p = 2(\text{mm})$

+ Number of contacts: $Z_h = 4$

+ Screw step: $p_h = Z_h \times p = 4 \times 2 = 8(\text{mm})$

Test durability:

$$\sigma_{td} = \sqrt{\left(\frac{4F_a}{\pi d_1^2}\right)^2 + 3\left(\frac{T}{0.2d_1^3}\right)^2} \quad (10)$$

where F_a-axial force (N); T—dangerous torque on the dangerous cross-section of the

screw.

The dangerous torque on the dangerous front is determined according to the formula:

$$T = \frac{F_a tg(\gamma + \varphi) d_2}{2} = 12.5 \times tg(0.25° + 3.64°) \times \frac{7}{2} = 2.97(\text{Nmm}) \quad (11)$$

$$\sigma_{td} = \sqrt{\left(\frac{4 \times 12.5}{3.14 \times 6^2}\right)^2 + 3 \times \left(\frac{2.97}{0.2 \times 6^3}\right)^2} = 0.46(\text{MPa}) \quad (12)$$

With stainless steel, $\sigma_{ch} = 205(\text{MPa})$, therefore,

$$[\sigma] = \frac{\sigma_{ch}}{3} = \frac{205}{3} = 68.33(\text{MPa}) \quad (13)$$

$\sigma_{td} < [\sigma]$ →Durable conditions are guaranteed.

Test stability:

To determine the softness of the screw, it is necessary to calculate the moment of inertia *J* and radius of inertia *i*:

$$J = \frac{\pi d_1^2}{4}\left(0.4 + 0.6\frac{d}{d_1}\right) = \frac{3.14 \times 7^2}{4} \times \left(0.4 + 0.6 \times \frac{8}{7}\right) = 41.762(\text{mm}^2) \quad (14)$$

$$i = \sqrt{\frac{J}{\pi d_1^2/4}} = \sqrt{\frac{41.762}{3.14 \times 7^2/4}} = 1.04 \quad (15)$$

Softness of screw:

$$\lambda = \frac{\mu L}{i} = \frac{2 \times 150}{1.04} = 288.46 \quad (16)$$

in which: $\mu = 2$ (screw is screwed in fixed-free style).

Using λ > 100the Euler formula to calculate the limit load, according to the Euler formula:

$$F_{th} = \pi^2 EJ/(\mu L)^2 \quad (17)$$

where *E* is the elastic modulus, for steel $E = 2.1.10^5(MPa)$; *J*—moment of inertia of the screw cross section.

$$F_{th} = \frac{3.14^2 \times 2.1 \times 10^5 \times 41.762}{(2 \times 150)^2} = 960.77(N) \quad (18)$$

Stable safety factor:

$$S_o = \frac{F_{th}}{F_a} = \frac{960.77}{10} = 96.077 > [S_o] = 2.5\ to\ 4 \quad (19)$$

Stable conditions are guaranteed.

Size of nut:

+ Height of nut: $H = \psi_H \times d_2 = 2 \times 7 = 14(mm)$

+ Number of thread turns of the nut $z = \frac{H}{p} = \frac{14}{2} = 7 < z_{max}$

+ Outside diameter of nut:

$$D \geq \sqrt{4F_a/(\pi[\sigma_K]) + d^2} = \sqrt{4 \times 12.5/(3.14 \times 40) + 8^2} = 8(mm) \quad (20)$$

select $D = 8(mm)$

+ Outside diameter of nut flange:

$$D_1 \geq \sqrt{4F_a/(\pi[\sigma_d]) + D^2} = \sqrt{4 \times 12.5/(3.14 \times 80) + 8^2} = 8(mm) \quad (21)$$

select $D_1 = 8(mm)$

Calculate and select the stepper motor:

Screw diameter: $d = 8(mm)$

Length of screw:$L = 150(mm)$

Thread step: $p = 2(mm)$

Distance traveled when the screw rotates once:

$$s = Z_h.p = 4.2 = 8(mm) \quad (22)$$

with Z_h—number of leads; p—screw thread pitch.

Maximum speed achieved by the structure: $v_{max} = 160\ (mm/s)$

→Angular velocity of Pulley when printing:

$$\omega_{in} = \frac{v_{max}}{R\dfrac{v_{max}}{d/2\dfrac{160}{4}(r/s)}} \quad (23)$$

→Time to complete 1 round of Pulley: $t = \frac{1}{40}(s)$.

Maximum speed of stepper motor:

$$V = \frac{s}{t} = \frac{8(mm)}{\frac{1}{40}(s)} = \frac{8(mm)}{\frac{1}{40} \times \frac{1}{60}(min()) \left(mm/min() \frac{19200}{8} (r/min()(r/min())) \right)} \quad (24)$$

The stepper motor chosen is Nema 17 (model KH4238-B90201) with a rated current of 1.2 A, and a voltage of 24 V.

Based on the graph of Figure 5 and the maximum rotation speed of the motor, $V = 2400(r/min)$. The torque of the stepper motor can determine $M = 75(mN.m)$.

The engine's capacity is:

$$P = V.M = 75 \times 10^{-3}.\frac{2400}{60} = 3(W) \quad (25)$$

where: V—engine rotation speed (r/s); M—torque (Nm).

The overall efficiency of the drive system is: $\eta = 0.95$.

Engine capacity:

$$P_{lv} = \frac{P}{\eta} = \frac{3}{0.95} = 3.15(W) \quad (26)$$

The 3D printer hydrogel with parameters follows in **Table 2**.

Table 2. 3D printer hydrogel parameter.

Parameter	Value
Print size	180 mm × 180 mm × 150 mm
Print head	2
Material volume/print head	20 mL
Print head diameter	0.6 mm
Speed extrusion	20–80 mm/s
Printing speed	10–90 mm/s

4. Fabrication and experiment

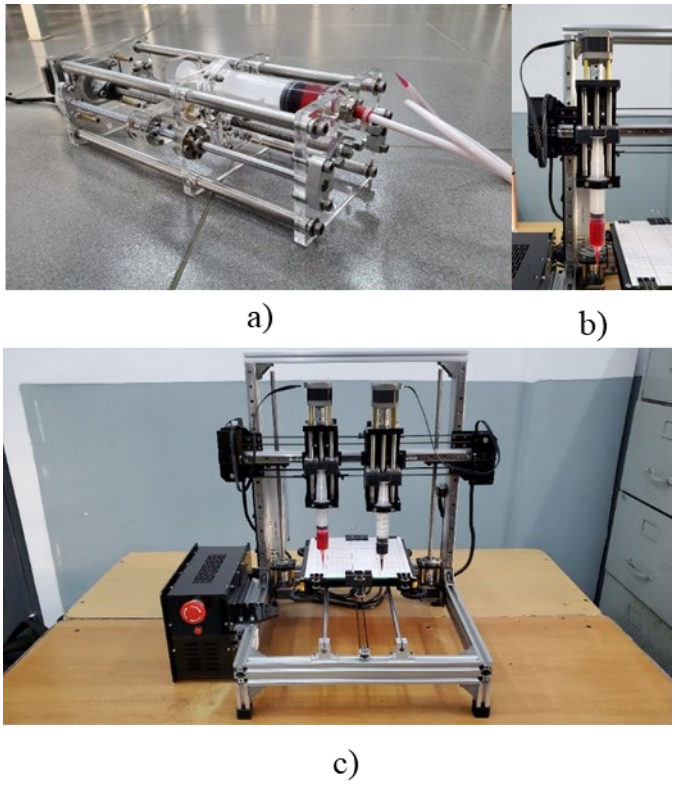

Figure 7. (a) Indirect extruder; **(b)** direct extruder; **(c)** dual direct extruder 3D printer.

After the design and manufacture of the 3D hydrogel material printer machine based on design and calculation results, it underwent evaluation for stability criteria (**Figure 7**). The machine frame ensures strong bearing capacity for the moving mechanisms of the *X*, *Y*, and *Z* clusters. The results demonstrate that the manufactured products meet the specified requirements (as **Table 2**). Following the verification of stable machine hardware operation, the machine is loaded with gel into the extruder and subjected to testing using both the direct and indirect extrusion methods, as shown in **Figure 8**. Test results show that hydrogel material can be completely printed on a 3D printer. Both direct and indirect extrusion heads provide good results. However, to evaluate the efficiency and optimal parameters of direct and indirect extruders, more in-depth research is needed.

Figure 8. Test results with indirect extruder and indirect extruder.

Assessment of the electrical conductivity of the hydrogel material 5% by weight of sodium alginate + 5% by weight of activated carbon through 3 test samples with different lengths (**Figure 9**). The result is shown in **Table 3**.

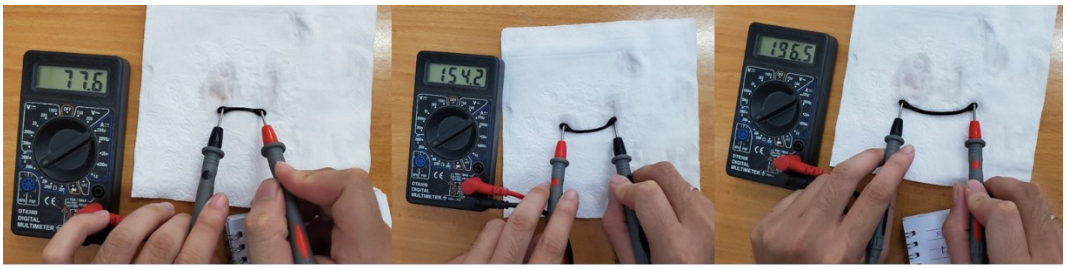

a b c

Figure 9. Conductivity measurement. **(a)** Sample 1; **(b)** sample 2; **(c)** sample 3.

Table 3. The result of the conductivity sample.

Item	Sample 1	Sample 2	Sample 3
Resistor R (kΩ)	77.6	154.2	196.5
Length l (mm)	34	50	67
Diameter d (mm)	2	2.3	2.7
Section A (mm^2)	3.14	4.16	5.73
Conductivity σ (s/m)	1.375×10^{-3}	1.347×10^{-3}	1.950×10^{-3}

Average conductivity:

$$\overline{\sigma} = \frac{\sigma_1 + \sigma_2 + \sigma_3}{3} = \frac{1{,}375 + 1{,}347 + 1{,}950}{3} \times 10^{-3} = 1{,}559 \times 10^{-3}(s/m)$$

Error:

$$a = |\overline{\sigma} - \sigma_1| = |1{,}558 - 1{,}375| \times 10^{-3} = 0{,}000183$$

$$b = |\overline{\sigma} - \sigma_2| = |1{,}558 - 1{,}347| \times 10^{-3} = 0{,}000211$$

$$c = |\overline{\sigma} - \sigma_3| = |1{,}559 - 1{,}950| \times 10^{-3} = 0{,}000394$$

$$d = \frac{a + b + c}{3} = \frac{0.000183 + 0.000211 + 0.000394}{3} = 0.000263$$

Conductivity:

$$\sigma = \overline{\sigma} \pm \mathrm{d} = 1{,}558 \times 10^{-3} \pm 0{,}000263(\mathrm{S/m})$$

Factors such as the type of hydrogel, the composition ratio, and the shaping method can significantly influence the conductivity of hydrogels. Previous studies

have supported this. By changing the concentration of PAA, the ionic conductivity (up to $35.36 \pm 7.72 \times 10^{-3}$ S.cm^{-1}). A PPy-based microfluidic hollow hydrogel fiber, which combines sodium alginate and polyacrylamide, has a conductivity of 0.32 S m^{-1}, based on the Fe^{3+} triggered simultaneous polymerization of pyrrole and bio adhesive dopamine on hyperbranched polymer chains, a paintable hydrogel with conductivity ($6.51 \pm 0.12 \times 10^{-4}$ S.cm^{-1} [20]. The hydrogels' extremely high apparent electrical conductivity is a result of their heterogeneous structure's thoughtful construction of 1.66×10^{-4} S.m^{-1} [21].

5. Conclusions

The 3D printer is capable of fully accommodating the 3D printing of hydrogel materials while meeting the parameters set in the original design. It has been tested for both indirect and direct extrusion methods, with the results demonstrating the printer's ability to work with hydrogel materials. The 3D printer is manufactured with parameters: 180 × 180 × 150mm working space, dual print head, 20 mL material volume, 0.6 mm nozzle diameter, 20–80mm/s in speed extrusion, and 10–90mm/s in printing speed.

The printer's ability to produce high-quality conductive hydrogel prints paves the way for further exploration of 3D-printed hydrogel-based materials. Conductive hydrogels offer a promising avenue for ongoing research, particularly in the development of biomedical sensors and electrically conductive biomaterials

Additionally, future studies should focus on further evaluating the optimal parameters for direct and indirect extrusion. The successful development of a 3D printer for hydrogel materials establishes a solid foundation for future research and can be extended to similar materials.

Author contributions: Conceptualization, TTN and VTT; methodology, NHP; software, HST and LNC; validation, TTN; formal analysis, NHP, HST and LNC; investigation, HST and LNC; resources, VTT; data curation, HST and LNC; writing—original draft preparation, NHP and TTN; writing—review and editing, THNP; visualization, THNP; supervision, VTT and QBP; project administration, TTN and VTT; funding acquisition, QBP. All authors have read and agreed to the published version of the manuscript.

Funding: This work belongs to project grant No: T2023-105 funded by Ho Chi Minh City University of Technology and Education, Vietnam. We extend our gratitude to the materials testing laboratory, Faculty of Mechanical Engineering, Ho Chi Minh City University of Technology and Education for their provision of the necessary equipment and machinery for the successful execution of this project. Additionally, we would like to thank the reviewers and editors for their constructive comments and suggestions for improving our work.

Conflict of interest: The authors declare no conflict of interest.

References

1. Tran VT, Mredha MdTI, Na JY, et al. Multifunctional poly(disulfide) hydrogels with extremely fast self-healing ability and

degradability. Chemical Engineering Journal. 2020; 394: 124941. doi: 10.1016/j.cej.2020.124941
2. Tran VT, Mredha MdTI, Jeon I. High-water-content hydrogels exhibiting superior stiffness, strength, and toughness. Extreme Mechanics Letters. 2020; 37: 100691. doi: 10.1016/j.eml.2020.100691
3. Nguyen TT, Tran VT. Long Nhut-Phi Nguyen, et al. A study on mechanical properties of Ca-alginate hydrogels. In: Proceeding of the 6th International Conference on Green Technology and Sustainable Development (GTSD); 2022.
4. Tran VT, Xu X, Mredha MdTI, et al. Hydrogel bowls for cleaning oil spills on water. Water Research. 2018; 145: 640-649. doi: 10.1016/j.watres.2018.09.012
5. J Wang J, Liu Y, Zhang X, et al. 3D printed agar/ calcium alginate hydrogels with high shape fidelity and tailorable mechanical properties. Polymer. 2021; 214: 123238. doi: 10.1016/j.polymer.2020.123238
6. Thien NC, Phuoc VV, Trinh PTD. Hydrogel materials—Properties and potential applications. Vietnam Science and Technology. 2019; 1-2.
7. Pham DTM, Hoang HT, Dang VD, et al. Preparation of bio - adhesive hydrogel based on chitosan for wound sealant. Science and Technology Development Journal. 2015; 18(2): 88-95. doi: 10.32508/stdj.v18i2.1136
8. Sano K, Ishida Y, Aida T. Synthesis of Anisotropic Hydrogels and Their Applications. Angewandte Chemie International Edition. 2018; 57(10): 2532-2543. doi: 10.1002/anie.201708196
9. Kopets E, Karimov A, Scalera L, et al. Estimating Natural Frequencies of Cartesian 3D Printer Based on Kinematic Scheme. Applied Sciences. 2022; 12(9): 4514. doi: 10.3390/app12094514
10. Huang CY. Extrusion-based 3D Printing and Characterization of Edible Materials. Elsevier. 2018.
11. Shahrubudin N, Lee TC, Ramlan R. An Overview on 3D Printing Technology: Technological, Materials, and Applications. Procedia Manufacturing. 2019; 35: 1286-1296. doi: 10.1016/j.promfg.2019.06.089
12. Jakus AE. An Introduction to 3D Printing—Past, Present, and Future Promise. 3D Printing in Orthopaedic Surgery. Published online 2019: 1-15. doi: 10.1016/b978-0-323-58118-9.00001-4
13. Jadhav A, Jadhav VS. A review on 3D printing: An additive manufacturing technology. Materials Today: Proceedings. 2022; 62: 2094-2099. doi: 10.1016/j.matpr.2022.02.558
14. Liu C, Xu N, Zong Q, et al. Hydrogel prepared by 3D printing technology and its applications in the medical field. Colloid and Interface Science Communications. 2021; 44: 100498. doi: 10.1016/j.colcom.2021.100498
15. Goyanes A, Allahham N, Trenfield SJ, et al. Direct powder extrusion 3D printing: Fabrication of drug products using a novel single-step process. International Journal of Pharmaceutics. 2019; 567: 118471. doi: 10.1016/j.ijpharm.2019.118471
16. Singamneni S, Behera MP, Truong D, et al. Direct extrusion 3D printing for a softer PLA-based bio-polymer composite in pellet form. Journal of Materials Research and Technology. 2021; 15: 936-949. doi: 10.1016/j.jmrt.2021.08.044
17. Van Damme L, Briant E, Blondeel P, et al. Indirect versus direct 3D printing of hydrogel scaffolds for adipose tissue regeneration Lana Van Damme, Emilie Briant, Phillip Blondeel, Sandra Van Vlierberghe. MRS Advances. 2020; 5(17): 855-864. doi: 10.1557/adv.2020.117
18. Cai J, Zhang B, Zhang M, et al. Indirect 3D printed ceramic: A literature review. Journal of Central South University. 2021; 28(4): 983-1002. doi: 10.1007/s11771-021-4674-1
19. Naghieh S, Sarker M, Sharma NK, et al. Printability of 3D Printed Hydrogel Scaffolds: Influence of Hydrogel Composition and Printing Parameters. Applied Sciences. 2019; 10(1): 292. doi: 10.3390/app10010292
20. Liang Y, Qiao L, Qiao B, et al. Conductive hydrogels for tissue repair. Chemical Science. 2023; 14(12): 3091-3116. doi: 10.1039/d3sc00145h
21. Zhou Q, Lyu J, Wang G, et al. Mechanically Strong and Multifunctional Hybrid Hydrogels with Ultrahigh Electrical Conductivity. Advanced Functional Materials. 2021; 31(40). doi: 10.1002/adfm.202104536